An Attempt to Verify Some Theories of El Niño

T. P. BARNETT

Scripps Institution of Oceanography, La Jolla, Calif. 92093

(Manuscript received 11 May 1976, in revised form 4 April 1977)

ABSTRACT

Numerous hypotheses have been proposed to explain interannual changes in equatorial water temperatures. It is shown that many of these hypotheses can be tested by expressing them in terms of a statistical-dynamical model based on the heat balance equation. The ability of the resulting model to account for variance in a 20-year record of observed water temperature provides a hitherto unavailable, quantitative measure of the hypothesis consistency.

Field data were used in conjunction with the models to show that the following general conclusions are consistent with available observations: 1) The advective terms (both horizontal and vertical) in the heat balance equation account for 30–50% of the variance in records of interannual changes in near-equatorial SST. 2) The advective changes are closely related to significant changes in the trade wind field, particularly those occurring near the equator and just west of the dateline, as well as major changes in sea level across the entire Pacific Basin.

Specific hypotheses about interannual changes in water temperature were tested. The following conclusions were found to be consistent with the available data: 1) Eastward advection of heat by the North Equatorial Countercurrent is far more important (29% of the variance) to the heat balance of the eastern tropical Pacific than local heating or consequences of long-term variations in the Northeast Trades. 2) At Talara, Peru, 48% of the SST variance was predictable one month in advance using basin-wide fluctuations in sea level as predictors. This suggests the importance to the heat balance off Peru of eastward advection of heat by currents or wave phenomena. Of less importance (14%) was trans-equatorial flow across the Galapagos front. Upwelling induced by *local* changes in the wind stress was not important, on the interannual time scale, in the estimate of SST. 3) Temperature changes in the central equatorial Pacific (Christmas Island) were consistent with the mechanisms of local upwelling at the equator (25%) and advection from the east (33%).

1. Introduction

The last decade has witnessed an upsurge of scientific interest in El Niño. This event apparently has several definitions, the most popular of which connotes an unusual increase in surface water temperature off South America. By whatever definition one chooses, El Niño is generally acknowledged to be a phenomenon occurring along the west coast of South America that can cause large changes in the local meteorological, oceanic and biological regimes. It is now clear that strong El Niños are also associated with major ocean/atmosphere changes throughout the tropical Pacific Basin and beyond (e.g., Ramage, 1975; Namias, 1976).

The goal of the present paper was to test, statistically, some of the theories that have sought to explain major departures of equatorial surface temperature from the long-term mean (SST_{DM}). This has not previously been done, perhaps because the theories are vague, qualitative or based on very meager observations. Most of the theories concern themselves with brief warming events, i.e., El Niños, and neglect changes in SST that occur during cold epochs and/or during the majority of the historical record. Since none of the theories call for "intermittent" physics, the hypothesized physical processes should be operative at all times, and hence be representable with continuous statistical models.

The tests described here were done by constructing the pseudo-heat budget for a selected area or station retaining only the physical processes suggested by a particular hypothesis. Combinations of actual data sets were then used to represent these physical processes. Using the "linear systems" formalism described in Section 3 and the process representations, a statistical/dynamical hindcast model was constructed to account for the nonseasonal fluctuations in the SST record of three major oceanic regions. The model coefficients were found from a 20-year data record. The model was judged to possess *significant* skill in quantitatively hindcasting SST_{DM} fluctuations over the 20-year time period only if the particular theories were *consistent* with the observed changes in phase and amplitude.

Subsequent sections of this paper review briefly the theories to be tested, the statistical methods and the data. Final sections (4–6) describe the construction to the linear systems models and their ability to account for observed variance in three regions of the tropical Pacific.

2. Theories to be tested

The hypotheses to be tested in this paper are described briefly below for each of three regions. The list is not all inconclusive but does contain most of the venerable ideas that can be tested with the available data. Some of the newer ideas (e.g., McCreary, 1976; Hurlburt *et al.*, 1976) regarding the mechanisms of SST change cannot be tested with available data and are only mentioned as appropriate.

a. Eastern tropical Pacific region

Bjerknes (1961, 1966a) examined the data from the eastern tropical Pacific in some detail. He suggested that locally reduced winds will lead to a reduction of sea-to-air heat flux and thus a warming of the near-surface waters. More important, he concluded that an oceanwide weakening of the zonal component of the Northeast Trades for one to two consecutive years would lead to an increased eastward transport by the North Equatorial Counter Current (NECC). This increased transport would increase the reservoir of warm water in the region described above resulting in a deepening of the thermocline and an increase in thermobaric energy. Wyrtki (1973) followed up this idea by relating a sea level difference index of the NECC to the SST in the region off Central America. Namias (1973) simultaneously provided data which suggested that a decrease in the subtropical easterlies and presumably the Northeast Trades in the eastern Pacific preceded an increase in Wyrtki's NECC index, thus supporting Bjerknes' earlier contention.

b. Peruvian coastal region

Interannual fluctuations in equatorial water temperature have a major manifestation along the coast of South America south of the equator. Such changes, which are referred to as El Niño (warm water) or anti-El Niño (cold water), are well documented in Peru and hence it is little wonder that many explanations for changes in SST in this region have been offered. Some of the theories which are presently capable of being tested are considered below in order of increasing complexity.

1) "Local wind" mechanism

One of the simplest candidate mechanisms is that during El Niños, local reduction of the longshore wind stress can lead to a cessation of upwelling which, in turn, allows local heating to increase SST. These ideas appear in the writings of Wooster (1960), Bjerknes (1961, 1966a) and Wooster and Guillen (1974). Recently, Hickey (1975) and Wyrtki (1975) have suggested this hypothesis may not be true. This latter idea finds support in the data of Stevenson *et al.* (1969).

2) The "overflow" mechanism

Many of the authors cited above invoke the "overflow" mechanism to explain major SST changes off Peru (e.g., Wooster, 1960; Bjerknes, 1961, 1966a; Stevenson *et al.*, 1969; Wyrtki, 1975; Hickey, 1975). It is hypothesized that the oceanic front between the Galapagos and South America is ruptured, allowing a relatively shallow layer of warm, low salinity water to push south across the equator. The abrupt arrival of this warm water at the coast signals the beginning of El Niño. The processes that create this overflow are partially discussed by Bjerknes and discernable in hydrographic data (e.g., Tsuchiya, 1974; Wyrtki, 1975; Wyrtki, *et al.*, 1976). Within 100 km of the equator, trans-equatorial, thermohaline circulation with southward flow above the shallow thermocline and north ward flow below occurs. The flow of warm water is fed from the reservoir discussed above. The volume of the reservoir and the depth of the thermocline are modulated at interannual time scales by the transport of heat from NECC as suggested above. The result is a fluctuating pressure force directed southward across the equator. An opposing force at the equator is the northward component of wind stress. An imbalance of the pressure/wind force system in favor of the pressure term leads to the southward overflow. Once across the equator, Bjerknes argues that the warm water is deflected eastward by the Coriolis force—an action that may be retarded or balanced by the local wind stress.

3) The "backflow" mechanism

In early papers, Bjerknes (1961, 1966a) suggests that a flux of warm water from the western equatorial Pacific plays an important role in the warming that accompanies El Niño events. Wyrtki (1975) expands this idea by proposing essentially two hypotheses: 1) Anomalous changes in the zonal component of the Southeast Trades change the circulation of the subtropical gyre of the South Pacific, particularly the South Equatorial Current (SEC). Higher than usual values of the wind stress result in a buildup of the east-west slope of sea level and an accumulation of water in the western Pacific. (Why this accumulation is not at least partially offset by stronger north/south flows near the western boundaries of the Basin is not discussed.) 2) As soon as the wind stress of the Southeast Trades relaxes from its previously high values, the water accumulated in the western Pacific will tend to move back to the east, perhaps as an equatorially trapped Kelvin wave (Lighthill, 1969; Godfrey, 1975;

Hurlburt *et al.*, 1976). At any rate, the eastward-directed equatorial currents will be strengthened. Warm water accumulates in the eastern Pacific and an El Niño situation results.

c. The central equatorial Pacific region

Major changes in SST along the equator in the central Pacific are generally attributed to fluctuations in the zonal component of the Southeast Trades at the equator (e.g., Bjerknes, 1966a,b). When these trade winds extend north across the equator there is divergence of the Ekman drift and a subsequent upwelling of cool water. However, when the winds weaken the upwelling weakens and warming occurs. This process is aided in the near surface layer by geostrophic convergence due to the zonal slope of sea level across the Pacific Basin near the equator. The Ekman upwelling mechanism has both theory and indirect data (e.g., Knauss, 1959; Hires and Montgomery, 1972) to support it. But no one knows how much of the observed SST_{DM} variance can be accounted for by this mechanism.

Another mechanism that could cause SST changes in the central Pacific is fluctuations in the transport of cold water from water from South America by the South Equatorial Current. The general distribution of water temperature in the region (Fig. 1) and the result that major warming (cooling) occurs off the coast of South America long before it occurs in the central Pacific both suggest this mechanism could be important. This has been mentioned (Barnett, 1975; Hickey, 1975; Miller and Laurs, 1975), but it does not seem to have been pursued seriously in the literature. It should be noted that Rossby waves emanating from the South American continental margin could presumably induce the same effects in the central ocean (McCreary, 1976; Hurlburt *et al.*, 1976).

Additional mechanisms that could cause SST changes in the central Pacific include surfacing of the Equatorial Undercurrent (e.g., Taft and Jones, 1974; Stevenson and Taft, 1971) and meridional shifts in the North Equatorial Countercurrent. These processes could not be modeled by the simple approach used here (Section, 3) and so have not been quantitatively tested. There is however, substantial data to recommend them as potentially important.

3. Model building considerations

a. Theory

The basic framework of the models to be investigated is to consider that the equatorial (near) surface temperature (T) is governed by a linear differential equation in time in response to a series of time-dependent forcing functions (F_i), each of which represents a distinct physical process (e.g., sensible heat flux). It is well known in linear systems analysis (e.g., Jenkins and Watts, 1968) that the dependent variable T can be expressed as an appropriate convolution of the

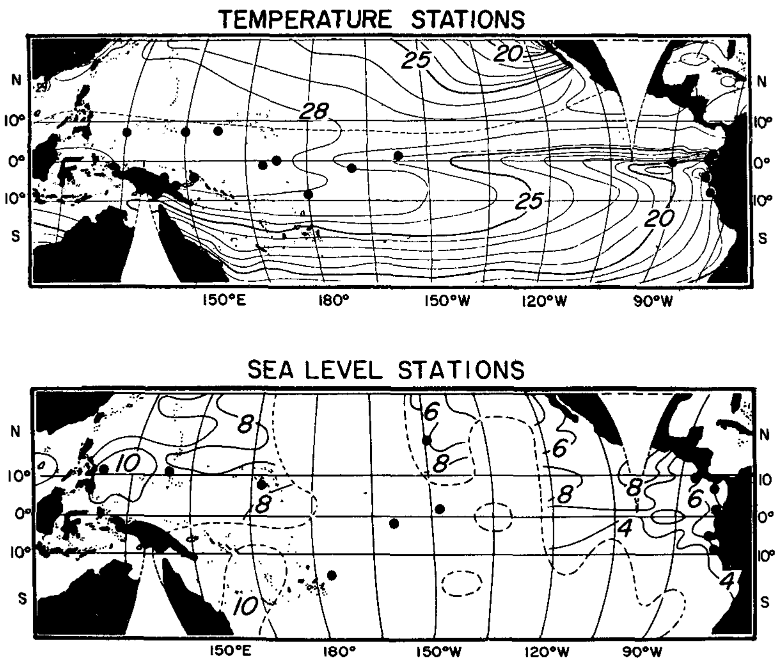

FIG. 1. Upper panel: sea surface temperature (SST) stations (solid circles) shown on the average annual SST distribution (°C). Lower panel: sea level stations shown on a map of the standard deviation (dyn cm) of dynamic height (after Wyrtki, 1974a).

forcing functions, i.e.,

$$\hat{T}(t)=\sum_i \int_0^\infty h_i(\tau)F_i(t-\tau)d\tau, \qquad (1)$$

where the $h_i(\tau)$ are weighting functions appropriate to time lag τ. The present value of $\hat{T}(t)$ depends only on combinations of F_i in times past. A special case of interest will be the situation of a single forcing function proportional to T itself. This situation represents a "persistence" prediction in which the behavior of T depends on its past history alone but with T at certain time lags weighted more heavily than others.

We wish to estimate the $h_i(\tau)$ by fitting Eq. (1) to actual data. These weighting functions completely characterize the behavior of the linear system. It is to be expected that the model (1) will in general not perfectly represent the actual data. Inadequacies in the measurements of the input/output series will also lead to errors. We assume the errors $Z=T-\hat{T}$ are random.

In order to obtain an "optimum" estimate of the temperature ($\hat{T}$), the functions $h_i(\tau)$ are chosen to minimize the mean-square value of the error term or

$$\langle Z^2(t)\rangle=\left\langle\left[T(t)-\sum_i \int_0^\infty h_i(\tau)F_i(t-\tau)d\tau\right]^2\right\rangle=\min, \qquad (2)$$

where the angle braces denote an ensemble average. The problem was simplified by assuming

$$h_i(\tau)=h_{ij}\delta(\tau-\tau_j)$$

such that

$$\int_0^\infty h_i(\tau)F_i(t-\tau)d\tau=\sum_j h_{ij}F_i(t-\tau_j).$$

The estimates of h_{ij} can be found directly using least-squares methods.

Assuming the $h_i(\tau)$ to be delta functions is in a sense restrictive, since it allows the system output to differ from the input by only a simple gain factor and phase shift. Yet the assumption is necessary in the present work to maximize the degrees of freedom in the statistical models thereby allowing meaningful tests of theory (see below).

The relative goodness or skill in making a model of the process $T(t)$, i.e., a hindcast, can be expressed in several ways. The skill measure (S_H) chosen for use in this paper is the percent of variance accounted for by the model, i.e.,

$$S_H=\left[1-\frac{\langle(T-\hat{T})\rangle}{\langle T^2\rangle}\right]\times 100, \qquad (3)$$

where both T and $\hat{T}$ have a zero mean value. Hence, a skill of 100% indicates a perfect prediction, while a value of 0 is equivalent to calling for a null predictand. Since we will be working exclusively with anomalies, the zero skill is equivalent to a hindcast of climatology.

Both Lorenz (1958) and, more recently, Davis (1976) point out the folly of using too many predictors in estimating T. In the case of hindcast, one is apt by chance to find a spurious relationship between the predictand and one or more predictors that lead to an apparently good representation of the subject data set. This artificial skill (S_A) may be estimated directly and related to S_H since

$$S_H=S+\frac{1}{N}\sum_i^M \frac{\tau_i^*}{\Delta t}=S+S_A. \qquad (4)$$

Here S is the "true" predictability skill obtainable from a perfect knowledge of the parent population, N the number of sample data points observed at time increments Δt, M the number of predictors (forcing functions) used in estimating T in Eq. (2), and τ_i^* an integral time scale associated with the ith forcing function (Lorenz, 1958; Davis, 1976) and directly estimatable from the data. Note also that S_A accounts for the fictitious modeling skill of a process for which a relatively few realizations are represented in the data (e.g., equatorial SST records).

In evaluating the models of Sections 4–6 the key numbers to watch are the estimate of the hindcast skill S_H and the artificial skill S_A of the model reconstruction. The ratio of the two skill numbers provides a relative, but quantitative, measure of the theory being tested.

It should be remembered clearly that the models and their evaluation are statistical in nature and thus can neither prove or disprove a selected theory. Nevertheless, the results provide a measure of the amount of SST_{DM} variance accounted for by each theory. The reader can thus obtain at least an idea of the degree of *consistency* between the observations and the various hypotheses during the time period covered by the data. This simple consistency check has not previously been available for the theories discussed below.

b. Sources of data

The sea surface temperature data from the islands and coastal stations (Fig. 1, Table 1) were reported in *Monthly Climatic Data for the World* (EDS/NOAA, 1950–70) *Surface Water Temperature and Density* (NOS/NOAA, 1950–70). The information represents monthly means of daily data for the period 1950–70. In most cases the observations were made on the majority of days in the month. Additional information for South America and the Galapagos was kindly provided by Mr. E. Forsbergh of the Inter-American Tropical Tuna Commission, La Jolla. Data for the Marsden square immediately off Central America were obtained from ship observations as summarized in the "Marine Deck" (TDF11).

It was found early in this study that anomalous temperature changes in the western Pacific were much smaller than those in the eastern Pacific. Further, their statistical properties were in many cases not different from uncorrelated noise. In view of these facts, plus the desire to concentrate on the eastern/central ocean, SST data west of 180° have not been used in this study.

The data on the equatorial Pacific trade wind systems were provided through the courtesy of K. Wyrtki. The data originally came from ship observations as recorded in the Marine Deck. These data were summarized by month for regions of dimension 2° latitude by 10° longitude. The areal coverage was between 30°N and 30°S and zonally over the entire Pacific Ocean. The data describe the time history of the (U,V) components of the trades between 1947 and 1972. The details of the extraction, editing, etc., can be found in Wyrtki and Meyers (1975).

The annual average distribution of the U and V components of the trade winds and their standard deviations are shown in Fig. 2. The core regions of both the Northeast and Southeast Trades are well-defined by the map of average U (negative to the west). The map of V (positive to the north) clearly shows the average position of the equatorial convergence zone ($v=0$), plus demonstrating the fact that the maximum in the V field occurs near the continents, not in mid-ocean. The standard deviations for the components are one-half to one-third their average value. The largest variations occur on the fringes of the high-speed regions, particularly in the western Pacific (U) and the eastern Pacific (V).

The large amount of information on the trade wind field has been represented by a set of empirical orthogonal functions (e.g., Lorenz, 1958; Kutzbach, 1967) to facilitate the modeling process. The details of this analysis, plus a description of the trade wind variations, are presented elsewhere (Barnett, 1977). One of the results of that study was to show that most of the variance in the wind field was statistically equivalent to incoherent noise. Although some filtering is done in later model tests, the high noise levels suggest that models will give a lower limit on the amount of variance accounted for by wind-associated mechanisms.

Sea level data came from the standard publication of what is now the National Ocean Survey Group of NOAA [User's Guide to NODC's Data Services (NOAA, 1974)]. The data had previously been developed in monthly time series form between 1950–70 by Wyrtki for a set of papers on sea level/dynamic height in the equatorial Pacific (1974a,b). Since several of the records contained gaps and/or were non-overlapping, it was useful to develop regional or composite sea level time series. In all cases, the intra-regional cross correlations were high enough (⩾0.8) to justify the regional representativeness of a single station. The stations used in the analysis are shown (Fig. 1) on a map of standard deviation of dynamic height from Wyrtki (1974a) to illustrate that their locations are representative of the principal fluctuations of the sea level field. Perhaps more importantly, the station data, although limited and not evenly distributed with respect to the equator, appear to provide a gross picture of sea level variability across the Pacific based on recent studies by Wyrtki (1977). This is certainly not the case with meteorological conditions. The details of the data and the regional definitions are given in Table 2.

The description of equatorial sea level fluctuations has been expanded and generalized by representing the anomaly field in terms of empirical orthogonal functions. This makes it possible to efficiently describe and use for modeling purposes the oceanwide variation of the field. The results of the analysis are interesting albeit tentative due to the paucity of data. The first three functions, accounting for 67% of the variance, are shown in the upper portions of Fig. 3. The station spacing clearly shows the contour patterns to be

TABLE 1. Characteristics of SST data set.

Station	Location	Time span
Buenaventura, Col.	4°N, 77°W	1953–70
Tumaco, Col.	2°N, 79°W	1951–70
Talara, Peru	4°S, 81°W	1942–70
Puerto Chicama, Peru	7°S, 80°W	1925–70
Galapagos, Ecuador	1°S, 90°W	1951–70
Christmas Island	2°N, 157°W	1954–70
Canton Island	3°S, 172°W	1951–67
Funafuti	9°S, 179°E	1951–70
Tarawa	1°N, 173°E	1951–61
Ocean Island	1°S, 170°E	1951–61
Ponape Island	7°N, 158°E	1951–61
Rabaul	4°S, 152°E	1951–61
Truk	7°N, 151°E	1951–70
Lae	7°S, 146°E	1951–61
Mandang	5°S, 146°E	1951–61
Koror	7°S, 134°E	1951–61

TABLE 2. Characteristics of sea level data set.

Station	Location	Time span	Regional grouping
Buenaventura, Columbia	4°N, 77°W	1950–69	1
Balboa, Panama	9°N, 80°W	1950–69	1
Pt. Armuelles, Panama	8°N, 83°W	1951–68	1
La Libertad, Ecuador	2°N, 81°W	1950–69	2
Talara, Peru	4°S, 81°W	1950–69	2
Christmas Island	2°N, 157°W	1956–70	3
Canton Island	3°S, 172°W	1950–67	3
Honolulu, Hawaii	21°N, 150°W	1950–71	4
Kwajalein	9°N, 168°E	1950–71	5
Guam, Mariana Islands	13°N, 145°E	1950–72	6
Legaspi, Philippines	13°N, 124°E	1950–72	7
Pago Pago, Samoa	14°S, 171°W	1950–70	8

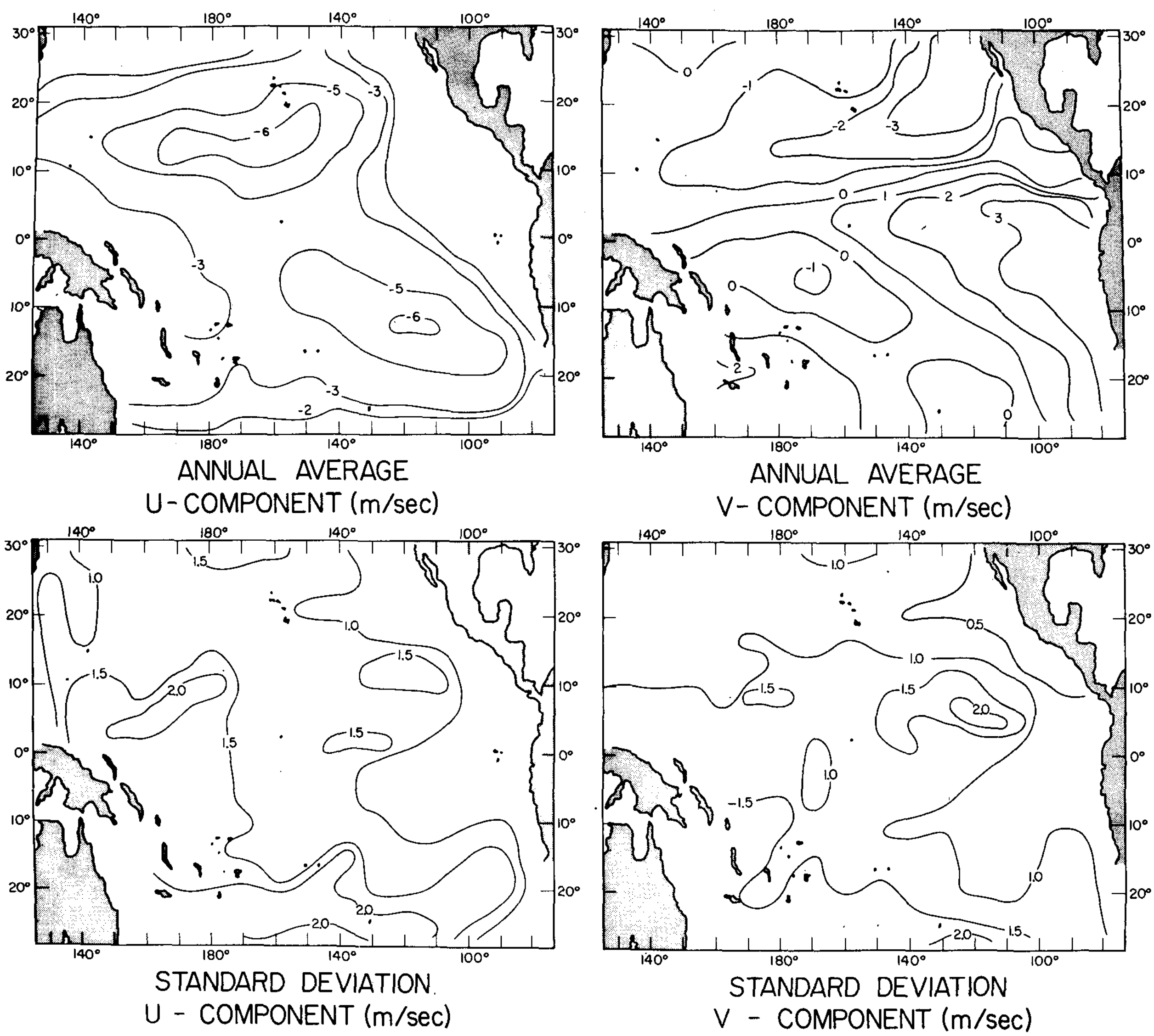

FIG. 2. Distribution of the long-term mean values of the U and V components of the trade wind field. Also shown are the standard deviations about the means. The -4 m s^{-1} contour was purposely omitted on the upper left panel.

schematic. The major features of the field are, nevertheless, clear. The first pattern (33%), represents variations, across the entire Pacific, in the mean east-west slope of the sea surface. It illustrates that the sea level fluctuations at the western and eastern margins are in antiphase. The nodal point for this half wave pattern lies near the dateline. The second function (19%) suggests a full wave pattern with simultaneous crests (or troughs) at the ocean margins. The associated trough (or crest) lies in the central Pacific, again near the dateline. The third pattern (15%) presents trans-equatorial variations occurring across the entire Pacific. The exact position of the 0 contour, if it were well known, could lead to some interesting interpretations of this pattern. The higher order patterns are associated primarily with the variability at individual stations and presumably represent local processes.

4. SST variations in the eastern tropical Pacific

The region roughly bounded by latitudes 0° and 10°N and longitudes 80°W and 100°W, i.e., the region extending some 1000 km west of lower Central America and Columbia, is much discussed in the literature (Section 2a). It is an area thought to spawn El Niños (e.g. Bjerknes, 1961; Wooster and Guillen, 1974; Hickey, 1975). Hence the dynamics causing SST change in this region could prove crucial to any model of large-scale equatorial air-sea interaction.

The predictant $T(t)$ was represented by ship reports from the region between 5–10°N and 80–90°W. The data were averaged by month by separate 5° squares over the period 1950–70, anomalies computed and combined into monthly estimates of SST_{DM} in the region. This estimate of temperature anomaly correlates at 0.80 with nearby shore stations [Tumaco (2°N) and Buenaventura (4°N), Columbia].

The forcing functions called for by the theories of Section 2 were represented by the following:

1) Air-sea heat exchange (both sensible and latent) —F_1

The theory suggests that the principal variation is due to changes in the strength of the local wind. Using typical formulations for the bulk heat flux formulas (e.g., Friehe and Schmitt, 1977) gives $\hat{T}(t)\propto\delta Q\propto\delta|\mathbf{W}|=h_1F_1(t)$, where $\delta|\mathbf{W}|$ is the interannual variation in mean wind speed averaged over the geographic region described above and δQ is the resulting variation in air-sea heat exchange. The estimates of $\delta|\mathbf{W}|$ were obtained from the actual observations of the trade wind field described in Section 3b. The constant h_1 is found from the historical record.

2) Transport of warm water to the east by the NECC—F_2

Wyrtki (1973, 1974b) gives substantial evidence to support the assumption that the relative strength of the NECC can be deduced from the sea level difference between Christmas and Kwajalein Islands. Using this index, interannual variation in the horizontal transport of the NECC and the subsequent increase in SST is represented by

$$\hat{T}(t)\propto\delta(\text{Sea Level}_{\text{Chris}}-\text{Sea Level}_{\text{Kwaj}})=h_2F_2(t-\tau).$$

Considering the great horizontal distances between the area where the NECC index is estimated and the area where its effect is supposed to be felt implies the need for a time lag (τ) between the predictor and predictand. Using the typical values of the NECC speed (Kendall, 1970) suggests $\tau=3$ months, a value supported by correlation analysis and the earlier calculations of Wyrtki.

3) Low-frequency fluctuations in the Northeast Trades

Fluctuations in the zonal component of the Northeast Trades, i.e., the nonlocal changes in the wind, were represented by the empirical orthogonal functions (EOF's) of the anomalous U component of the trade wind field between 8–30°N. However, only those EOF's that were statistically different from incoherent noise were retained for the index (Barnett, 1977). This is equivalent to low-pass filtering the wind field to remove noise that might otherwise obscure long-period interactions with the ocean. The physical assumption behind the filtering was that the large mismatch in time scale between the high-frequency noise forcing functions and the low-frequency SST_{DM} signal would result, at best, in a very weak coupling between the two fields.

The time integral effect involved in Bjerknes' ideas was represented in the following manner. The autocorrelations of the EOF's all had effective first zero crossings at time lags of order 3 months. Thus, non-

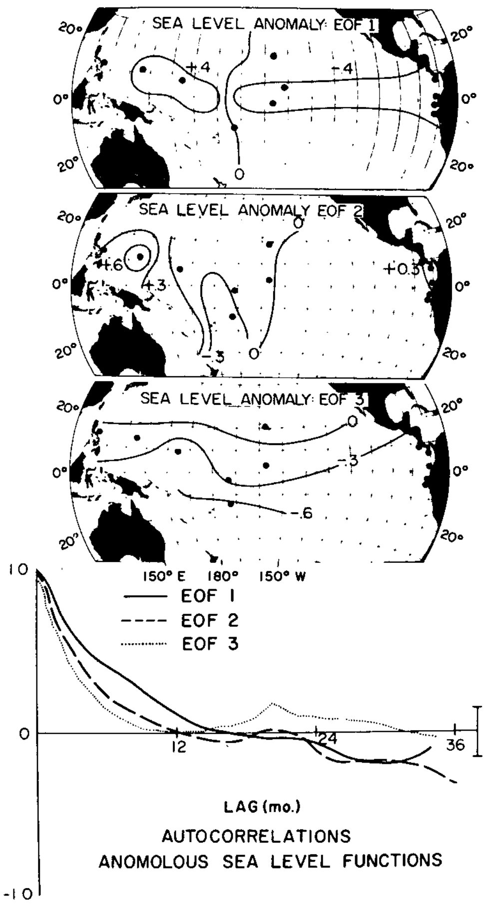

FIG. 3. The upper panels show the first three empirical functions for interannual sea level fluctuations. The lower panel shows the autocorrelation for each of the associated amplitude functions.

overlapping averages of the EOF's over 3-month periods represent quasi-independent estimates of the field variability. These averages, computed over the period one year prior to hindcast time, served as predictors. This results in four EOF predictors and the hindcast relation

$$\hat{T}(t_0)\propto\sum_{i}^{3}\sum_{j=0}^{3}\Big[\tfrac{1}{3}\sum_{k=1}^{3}A_i(t_0-t_j-k\Delta t)\Big]=\sum_i\sum_j h_{ij}F_i(t_0-t_j),$$

with $t_j=3j$, $j=0, 1, 2, 3$ and $\Delta t=1$, all units in months. The amplitude function $A_i(t)$ represents the strength of the ith EOF (e.g., see Lorenz, 1958).

The statistical test, then, should determine if all four seasons for a given EOF are equally effective as predictors. If this were the case, the hypothesis would be consistent with the data. If none of the predictors are useful in the hindcast, one could conclude that the hypothesis and the data are inconsistent.

TABLE 3. Hindcast skill (%) for eastern tropical Pacific SST_{DM}*.

Overall skill without persistence	F_2 alone	Persistence	NECC and persistence
41 (20)	32 (3)	47 (4)	61 (7)

* Value of S_A are given in parentheses in this and all remaining tables.

RESULTS

The resulting hindcast equation combined terms 1–3 and, when solved, gave a skill (S_H) for predicting T shown in Table 3. Also shown in the table, in parentheses, are the values of "artificial skill" (S_A) expected for each simulation, as well as the skill obtainable from a persistence model with a 3-month lag. The time history of T and $\hat{T}$ are shown in Fig. 4 for two selected simulations. A number of conclusions are apparent:

1) All values given in Table 3 exceed the estimates of artificial predictability. Thus, there seems to be validity to at least some aspect of the model being tested.

2) A close examination of the contributions of each mechanism reveals that the NECC transport idea (F_2) is responsible for virtually all of the real hindcast skill. This advective process is thus of considerable importance in the eastern tropical Pacific. However, a close inspection of Fig. 4 will show that the hindcast based solely on this mechanism has some consistent and significant shortcomings. There are obviously other terms important to the budget that have not been included in the model.

3) The indices of long-term fluctuations in the Northeast Trades covering the entire year prior to hindcast time, by themselves, gave values of $S_H \approx S_A$. Thus the long period of reduced winds envisaged by Bjerknes is not strictly consistent with the data. Examining the suggested relation on a season-by-season basis, however, revealed that fluctuations in the wind field 4 and, particularly, three seasons prior to hindcast time contributed approximately two times more to the variance than expected by chance (i.e., $S_H = 2S_A$). This 7–12 month lag is in agreement with the suggestion of Namias discussed above. Unfortunately, the estimated true skill contributed to the hindcast by any combination of Northeast Trades indices was less than 10%. It may be concluded that low-frequency fluctuations in the Northeast Trades do precede changes in eastern tropical SST_{DM} by 0.5–1 year but that these fluctuations cannot be used directly to explain a significant portion of the SST_{DM} record.

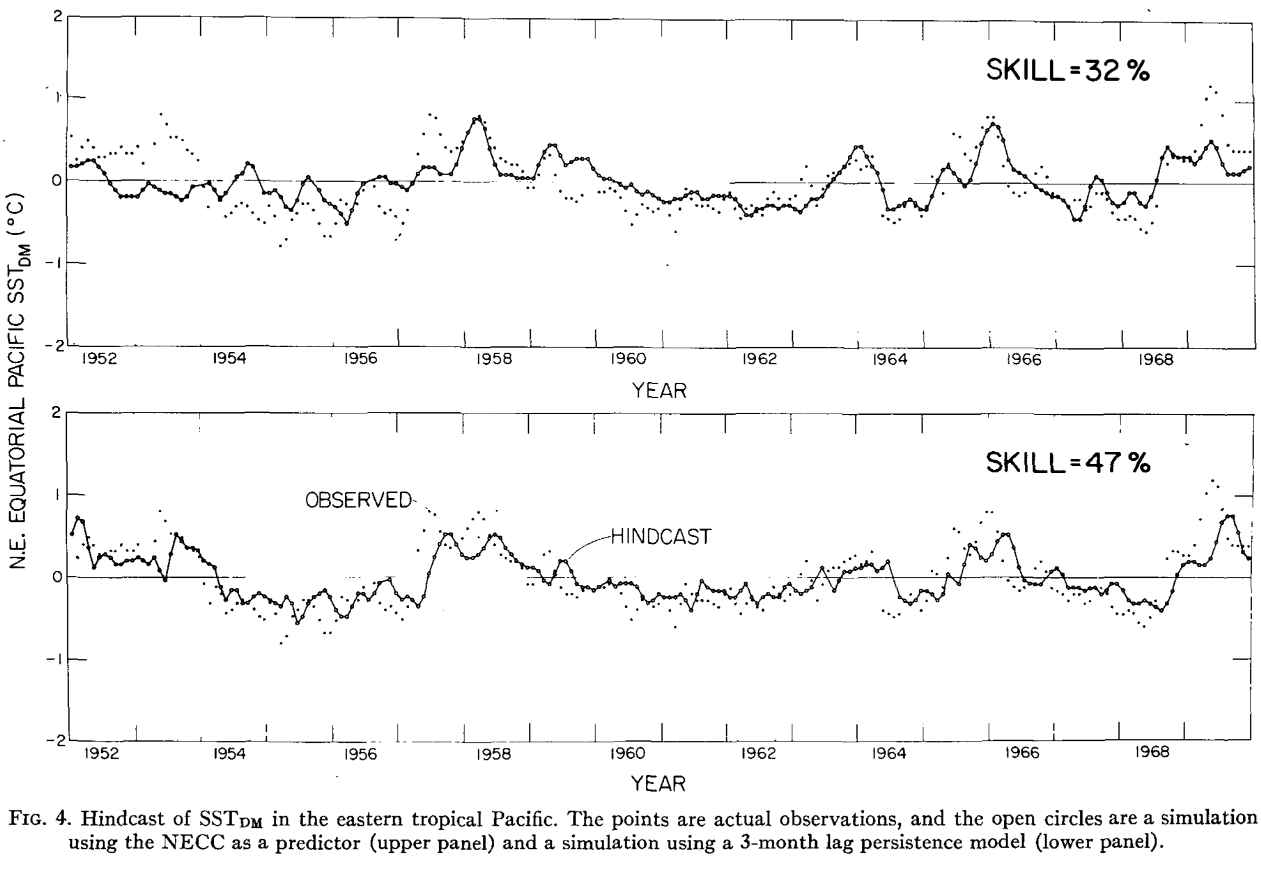

FIG. 4. Hindcast of SST_{DM} in the eastern tropical Pacific. The points are actual observations, and the open circles are a simulation using the NECC as a predictor (upper panel) and a simulation using a 3-month lag persistence model (lower panel).

4) Local variations in the heat flux (F_1), as estimated here, contribute only 4% to the hindcast skill, a value that is close to that expected by chance. This suggests that anomalous heat flux is not a major cause of fluctuations in SST_{DM}.

5) The results of a persistence model (Table 3) show that persistence accounts for more variance than the NECC predictor. Unfortunately, the persistence hindcast, because of its built-in 3-month lag cannot correctly estimate critical turning points in the time series and, therefore, is not practically useful. The NECC hindcast, while less accurate, correctly captures the temporal occurrence of major peaks and troughs in the SST record (Fig. 4).

5. Peruvian coastal region

The interannual fluctuations of temperature along the coast will be represented by data from Talara (4°S). This station is extremely well-correlated with its sister stations, e.g., 0.89 with Puerto Chicama (7°42′S), and will be taken as representative of the Peruvian coastal region. It is apparently also representative of nearby oceanic conditions on monthly time scales since Talara SST_{DM} correlates well (0.72) with SST_{DM} at the Galapagos Islands which are some 1000 km to the northwest.

a. *The "local wind" mechanism*

This mechanism, as described in Section 2b, is modeled quite simply by

$$\hat{T}(t) \propto \delta\tau_y(t),$$

where the forcing function $\delta\tau_y$ is the anomalous northward component of the wind stress *near the coast*, the y axis in this case being parallel to the coast. Considering the process involved, the results of the coastal upwelling studies (e.g., Barton *et al.*, 1976; Huyer *et al.*, 1974) and the sampling interval of the data, there should be no detectable time lag between changes in $\delta\tau_y$ and T and hence the input-output functions are simultaneous.

The validity of the "upwelling" model was tested using a 20-year time history of τ_y extracted from the trade winds data for geographic regions bounded by 1°N–10°S and 80–100°W and 2–6°S and 80–90°W. The hindcast skills in reproducing the time history of SST_{DM} at Talara were, respectively, 12 and 4% versus 4% expected by chance for each case.

It should be pointed out that the maximum correlation (0.46) between the variables suggests τ_y *lagged* SST_{DM} by four months, a result also found by Hickey (1975). Furthermore, the positive correlation indicated that *stronger* winds accompany warming events. The skill of this model may be contrasted with the skill of 49% obtained by using a persistence predictor one month in the past.

It may be concluded that local wind induced upwelling is not a highly significant process in changing SST off South America on interannual time scales. The devotees of this mechanism may well argue that the wind observations used in this test are crude and noisy and might, therefore, obscure a real relationship. To some extent this argument may be valid. Yet, as we shall see, the wind data do allow skillful hindcast using other hypotheses.

b. *The "overflow" mechanism*

A model designed to investigate the "overflow" hypothesis (Section 2b) relates a measure of the trans-equatorial flow to the SST_{DM} of Peru and has the following components:

1) The anomalous SST along, and just off the coast of Peru is again represented by the Talara station data. The recent observational results of Stevenson *et al.* (1969) and Wyrtki *et al.* (1976) show that Talara is spatially coherent with the frontal region during (at least) minor El Niño events.

2) The oceanic pressure gradient across the equator cannot be represented directly due to inadequate hydrographic data. As an alternative, the gradient will be represented as (i) the difference in monthly sea level heights (δH) between Buenaventura, Columbia (4°N) and La Libertad, Ecuador (2°S), and (ii) the sea level difference between Buenaventura and Talara. These differences represent the north-south gradient of sea level across the equator and should be an adequate measure of relative change of pressure gradient (Reid and Mantyla, 1976).

The first set of stations are located north of the front (Buenaventura) and in the frontal region, respectively. Talara, in the second set, is almost exactly between the south extremity of the frontal area and the intense upwelling region off Peru (Stevenson *et al.*, 1969). The stations are close enough to be reasonably well-correlated. The differencing operation thus removes basin-scale influences, leaving local fluctuations as desired.

The relation between either of the measures of trans-equatorial pressure gradient and temperature at Talara is thus

$$\hat{T}(t) \propto \delta H(t-\tau_1) = h_1 F_1(t-\tau_1).$$

The response of the temperature to this type of forcing should be rapid considering the short distances involved and the sampling interval of the data. A value of $\tau_1 = 1$ month, a number supported by the data of Wyrtki *et al.* (1976), was used in the tests discussed. Other reasonable time lags were tried but the results were essentially unaltered.

3) The force opposing the oceanic pressure gradient was supplied by the meridional component of wind stress near the equator (τ_y) and derived directly from the trade wind data. An areal integral representation

TABLE 4. Hindcast skill (%) for overflow model.

Lag (months)	F_1+F_2	Persistence	Persistence $+F_1+F_2$
1	20(6)	79(4)	79(9)

for this forcing term was obtained by averaging τ_y over the region between 2°N and 2°S and 80–100°W. This spatial averaging should help minimize the noise levels in τ_y thereby enhancing any low-frequency relationship that may exist with SST_{DM}. The same time lags noted above must be used in the expression relating $\hat{T}$ and the forcing function

$$\hat{T}(t) \propto \tau_y(t-\tau_1) = h_2 F_2(t-\tau_1).$$

4) Once south of the equator the Coriolis force to the east can be offset by the zonal component of the Ekman drift (i.e., the τ_y component of the wind stress off the coast of South America. We have already seen that this term is of negligible predictive value (Section 5a). This potential mechanism is thereby deleted from the present model. It may also be noted that available hydrographic data suggest the potential retarding force of the Peru Current seems unimportant within a few degrees of the equator (Tsuchiya, 1974; Bjerknes, 1966a) and this will also be neglected.

RESULTS

The model resulting from the combination of terms 1)–3) produces the hindcast skill shown in Table 4. These numbers refer to the hindcast using the Buenaventura/La Libertad pair of sea level stations. The Buenaventura/Talara set produced almost identical skill estimates. The skill obtained using persistence (one month lag) is also shown for comparison as are the estimates of artificial predictability (in parentheses).

The results suggest that the overflow process may be of significance in affecting the heat budget off Talara. Of particular importance in the hindcast was the estimate of the pressure gradient which accounted for two-thirds of the real skill. This suggests that local oceanographic, instead of atmospheric, effects control the SST_{DM}. This conclusion is in concert with that of the previous section but does not exclude the possibility that the local oceanic behavior is driven by remote atmospheric events.

It is clear that the majority of the variance in the Talara SST_{DM} record is *not* accounted for by the overflow mechanism as represented here. This suggests that transequatorial advection can contribute to the local heat budget but not in a dominant way.

c. The "backflow" theory—Phase 1

The first part of this hypothesis (Section 2b) calls for interannual fluctuations in the zonal component of the Southeast Trades to be accompanied by fluctuations in the zonal gradient of the Pacific Basin's sea level field; specifically a rise (or fall) in sea level in the western Pacific and presumably a corresponding fall (or rise) in sea level in the eastern Pacific. Note that the wind field fluctuations are *not* the local changes discussed above but rather refer to the properties of an entire trade wind system.

The sea level fluctuation is clearly represented by the first empirical function (A_1) of the sea level field (Fig. 3). The higher order functions are either of the wrong spatial scale or improperly oriented to represent the desired variation. The variation in the wind field was represented as the sum of the nonrandom amplitude functions derived from the EOF analysis of the zonal component of the trade wind field data between latitudes 8°N–30°S and longitudes 80°W–130°E, an area that encompasses the Southeast Trades and then some [see Barnett (1977) for more details]. The signal/noise discrimination was again based on the great mismatch in time scales between the noise terms, variations in sea level and the requirements of the hypothesis. Thus, the mathematical model is

$$A_1(t) = \sum_{i=1}^{3} h_i F_i(t-\tau).$$

The three forcing functions that balance the sea level gradient were the first, second and fourth EOF's of the zonal component of the regional trade wind field. The remaining EOF's were indistinguishable from incoherent noise.

RESULTS

Considering the type of force constituting the balance shown above implies $0 \leqslant \tau \leqslant 2$ months, depending on whether sea level responds in a barotropic mode or via a low order baroclinic mode (e.g., Godfrey, 1975; McCreary, 1976). The model was run for both time lags plus a 4-month lag and the results shown in Table 5. Simulations using negative values for τ had less skill than for $0 \leqslant \tau \leqslant 2$. An additional test, including the third, fifth and higher order EOF's of the regional trade wind field, showed these additional predictors added less to the hindcast variance than their expected artificial contributions, thus validating the *a priori* selection of the nonrandom components.

TABLE 5. Hindcast skill (%) for equatorial sea level fluctuations from trade winds.

Lag (months)	Trades	Persistence	Trades+ persistence
0	35(7)	—	—
2	35(7)	69(3)	73(10)
4	22(7)	38(3)	45(10)

The results of the EOF model apparently demonstrate the close, nearly simultaneous connection between interannual fluctuations in the large-scale behavior of the sea level field of the tropical Pacific Ocean and the fluctuations in the strength of the Southeast Trades, thus substantiating the Bjerknes/Wyrtki hypothesis. It should be noted that the measure of slope used here accounts for roughly one-third of the variance in the overall anomalous sea level field and about two-thirds of the variance associated with basinwide fluctuations (as opposed to variance associated with single stations).

Investigations of the individual contributions to S_H by the wind field EOF's shows the above result to be somewhat misleading. It turned out that most of the hindcast skill (26%) came from EOF1. This function is illustrated in Fig. 5 and clearly shows the important variability is not associated with core strength of the Southeast Trades system. Rather the region of principal variance in the pattern (the area within the -200 contour) occurs west of the dateline, along and just north of the equator. This area lies between and somewhat west of the high-speed regions of the trades. It is shown elsewhere (Barnett, 1977) that this variation is associated with an areal expansion (or contraction) of the two trades systems during which the speed minimum (Fig. 3) nearly disappears (or intensifies). This region also lies adjacent to, but not congruent with, the "equatorial dry zone" in which rainfall is highly correlated with, but *lags*, SST_{DM} at South America (Doberitz, 1967; Schütte, 1967). Thus atmospheric fields in the central Pacific appear to obey complex interrelationships which shall not be pursued here. At any rate, one can expect major changes in the easterlies just north of the equator and just west of 180° to precede major changes in general sea level structure of the Pacific Basin.

d. The "backflow" theory—Phase 2

The second part of the backflow hypothesis calls for the wind-induced alterations of the Equatorial Current System to alter the temperature field off South America by advection. Whether this change is the result of increased transport by the current systems or equatorially trapped wave events (e.g., McCreary, 1976; Hurlburt *et al.*, 1976) is not clear. Given this uncertainty, plus a limited data set, the best one can do is attempt to see if changes in the basinwide sea level field are strongly related to changes in SST off South America. Since there is clear evidence that sea level changes are closely related to changes in dynamic height (Wyrtki, 1974a) and since separate calculations (not shown here) indicate the EOF's of sea level are highly correlated with the Wyrtki indices of equatorial current strength, one might then infer that some type of flow-field alterations precede the South American SST_{DM}.

The model used was

$$\hat{T}(t) \propto \sum_{i=1}^{3} A_i(t-\tau) = \sum_i h_i F_i(t-\tau),$$

where the first three EOF's (A_i) of the sea level field (67% of the total variance) are used as predictors. Remember that the higher order functions depict local variance and, therefore, were neglected. Considering the different means by which the sea level signal might be transmitted and related to T suggests values of τ in the range 0–2 months. Cross-correlation analysis favored values of 0 or 1.

RESULTS

The results of the model for these time lags are shown below and graphically for $\tau=1$ month in Fig. 6. The illustration demonstrates that the hindcast captures the principal features of the Talara record, even to the "double peaks" associated with major El Niños. The major failings of the hindcast occur during two major cold spells (1954 and 1960) and the underestimation of the largest events. Values of $\tau>2$ months and less than zero gave much worse results than those shown in Table 6.

The results demonstrate a close coupling between

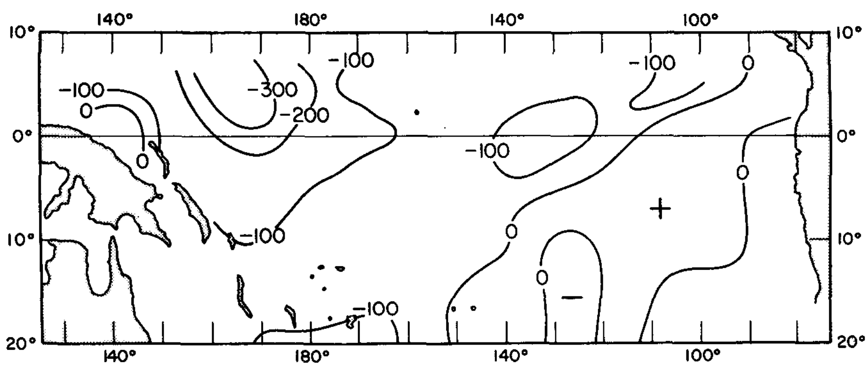

FIG. 5. First empirical orthogonal function of the anomalous zonal component of the trade wind field between 8 and 30°N.

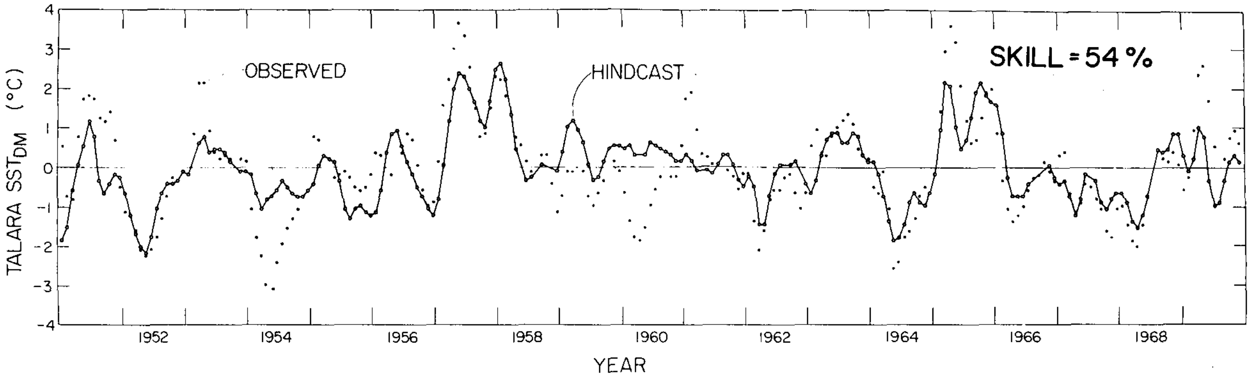

FIG. 6. Hindcast of Talara SST_{DM} from sea level EOF's 1–3 lagged one month.

changes in sea level across the Pacific Basin and SST_{DM} off South America. As stated above, the causal mechanism(s) responsible for the relation are not entirely clear. The results do, however, give a hint as to a mechanism. Note that EOF's 1 and 3 are considerably more valuable as estimators of T than is EOF 2. A review of the patterns associated with the EOF's (Fig. 3) suggests that the first and, particularly, the third patterns reflect, in a gross way, changes in the north-south slope of sea level. Fluctuations in the large-scale features of these slope patterns could thus be taken as indicators of zonal flow and geostrophic convergence/divergence near the equator.

Considerably more data will be required to completely understand the relationship between sea level, SST_{DM} and the zonal current regimes. For the time being, we may conclude that fluctuations in the basin-wide sea level field have considerable ability to predict SST_{DM} off the coast of Peru.

6. The central equatorial Pacific

A model that represents the mechanisms thought to cause temperature changes in the central Pacific (Section 2 c) has the following components:

1) The SST in the central equatorial region will be represented with data from Christmas Island (1°59′N). This station is well correlated (0.7) with the SST_{DM} at Canton Island (3°S) about 1500 km to the west and so should provide a good measure of the relative temperature changes in surrounding ocean area.

2) The strength of the equatorial upwelling is theoretically proportional to the zonal component of wind stress (τ_x) at the equator. The needed measure of τ_x was obtained by averaging the actual trade wind observations over an area bounded on the north and south by 2° latitude and between longitudes 130°W and 160°W. This averaging should help reduce the noise level in the time history of τ_x. The hindcast relation from basic Ekman theory is

$$\hat{T}(t) \propto \delta\tau_x(t-\tau_1) = h_1F_1(t-\tau_1).$$

The value of τ_1 was taken to be 1 month in concert with the previously published lag relation found between equatorial SST_{DM} and wind strength (Hires and Montgomery, 1972) and the results of the Coastal Upwelling Program (e.g., Holladay and O'Brien, 1975).

3) The transport of heat (or lack of cold water) from the east can be presented in several ways. The simplest approach is to assume that fluctuations in SST that occur at the coast of South America are transported intact to the central ocean, i.e.,

$$\hat{T}(t) \propto \text{Talara } SST_{DM}(t-\tau_2) = h_2F_2(t-\tau_2),$$

where $\tau_2 = 6$ months is obtained by dividing the distance between Talara and Christmas Islands by a typical speed for the South Equatorial Current (e.g., Cromwell and Bennett, 1959) or the typical speed of a first-mode Rossby wave.

TABLE 6. Hindcast skill (%) for Talara SST_{DM} from EOF's 1–3 of sea level anomaly field.

Lag (months)	EOF 1	EOF 2	EOF 3	Sum	Persistence	EOF's +Persistence
0	25(2)	8(2)	7(2)	41(6)	—	41(6)
1	26(2)	8(2)	19(2)	54(6)	79(4)	82(8)
2	17(2)	4(2)	16(2)	38(6)	45(2)	52(8)

RESULTS

The results of the two-component model are given in Table 7. The hindcast time series is compared with actual observations in Fig. 7. The agreement is good in most respects. Small variations in time lags that gave larger values of the τ's did not greatly effect the calculations. Variations that were negative (e.g., $\tau_i<0$) gave considerably worse results. The results obtained with a persistence model ($\tau=6$ months) are shown for comparison and again the "artificial" skill is shown in parentheses.

The skill of the hindcast is highly significant being nearly ten times that expected by chance. Both mechanisms, as represented, appear to be consistent with the observations. Note, however, that the sum of the individual skills of the (non-orthogonal) predictors is greater than their overall skill. The predictors are clearly interdependent. Thus the conclusion that both mechanisms are operative could be merely the result of this interdependence. To determine if, in fact, both mechanisms contributed significantly to the estimation of T, another set of hindcasts was run in which the predictors were orthogonalized. The results show that each mechanism is contributing significantly to the hindcast skill. It is concluded that each process is important to the heat budget of the central equatorial ocean.

7. Summary

An attempt has been made to determine if some of the hypotheses for changes in equatorial water temperature are consistent with available data. The approach was to construct a statistical model of anomalous SST fluctuations from considerations of linear systems theory and the heat balance equation. The skill of the models in reproducing a 20-year time history of SST_{DM} was taken as a measure of consistency between the modeled hypotheses and the actual observations for the period covered by the data.

The general results confirm statistically the following conjectures of earlier authors:

- Variations in the trades are associated with major adjustments in the basinwide sea level field. However, the wind variations are associated with geographic regions in the western Pacific and not with the high speed regions, i.e., the core of the trade wind systems.
- Sea level changes are highly useful predictors of SST. Since sea level changes are closely linked to dynamic height and the strength of the equatorial current system, it may be concluded that advection, both horizontal and vertical, is a dominant mechanism in the heat balance of the central and eastern equatorial Pacific. Local air/sea heat exchange does not seem to play a dominant role in the budget.

TABLE 7. Hindcast skill (%) for Christmas Island SST_{DM}.

F_1	F_2	F_1+F_2	Persistence	F_1+F_2+ Persistence
27(2)	36(3)	46(5)	18(4)	47(10)

The results lead to the following specific conclusions:

1) Observed interannual fluctuations of SST in the eastern tropical Pacific are consistent with a North Equatorial Countercurrent (NECC) transport mechanism hypothesized by Bjerknes/Wyrtki. The NECC mechanism accounts for 29% of the record variance which is a factor of 10 above the skill expected by chance. The results are inconsistent with the causal hypothesis of local heating and only weakly support a hypothesis that Northeast Trade Wind fluctuations precede major SST changes.

2) Observations of SST fluctuations in the Peruvian coastal zone are not consistent with the idea that locally driven upwelling, by itself, plays a significant role in the large-scale interannual variations in heat balance. The major, long-term variations in SST, i.e., those generally associated with El Niños, are evidently associated with other causes. This conclusion does not preclude the possibility that local wind-induced upwelling, among other factors, is a significant factor in the high-frequency fluctuations of the coastal heat storage field. It does suggest, however, that the local wind induced upwelling in the absence of other processes contributes only a small amount of variance (0–8%) to the monthly records of SST_{DM}.

On the other hand, the flow of warm water south across the equatorial front apparently has a significant, but *limited*, effect on the heat budget of the Peruvian

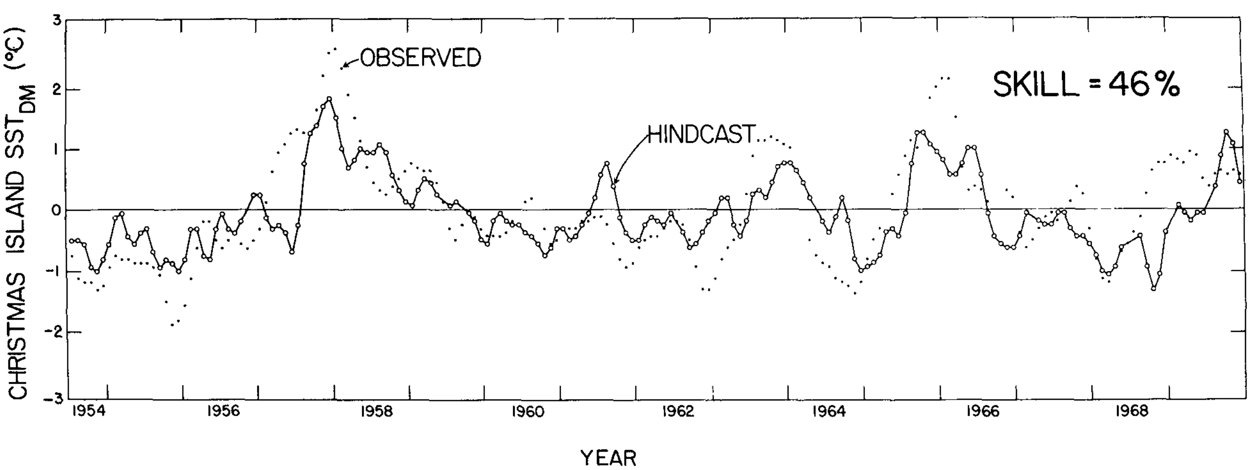

FIG. 7. Hindcast of Christmas Island SST_{DM} with the model of Section 6 as compared to actual observations.

coastal stations (14% of the variance). As represented here, this process cannot account for the major changes in SST_{DM} observed off Peru.

Interannual changes in the zonal components of the trade winds near the dateline and just north of the equator are closely associated with changes in the basin-wide sea level field and, hence, the zonal oceanic pressure gradient. The wind fluctuations precede those in the sea level field by 0–2 months. The fact that the main variation in these predictors occurs near the dateline as opposed to the eastern ocean is an unexpected finding that has apparently not been previously shown. The resulting changes in the sea level field, as represented here with EOF's, were successfully used to hindcast changes in SST_{DM} (48% of the variance) at the Peruvian coast, thus suggesting the importance of horizontal advection to the heat budget of that region. The hypotheses of Bjerknes (1966a) and more recently Wyrtki (1975), as represented here, are thus compatible with these latter results. But so are the somewhat different mechanistic hypotheses of McCreary (1976) and Hurlburt *et al.* (1976).

3) The heat balance of the central equatorial Pacific was found to be associated with local upwelling due to Ekman divergence at the equator and, more importantly, advection of "temperature signals" from the coast of South America. However, these processes together accounted for less than 50% of the observed variance, thus suggesting the importance of other (untested) terms in the heat budget equation.

Acknowledgments. Many thanks are due Bill Patzert, Jerry Namias and Jay McCreary for stimulating discussions during the course of this work. Particular thanks are due Russ Davis for his general encouragement and the unselfish manner in which he shared his ideas. Klaus Wyrtki and Eric Forsbergh provided unique data which made many of the analyses possible. Wyrtki, McCreary and Patzert provided valuable suggestions on first drafts of the manuscript.

This work was supported by the International Decade of Ocean Exploration as part of the NORPAX program (Contract OCE74-24592). The work was carried out under the auspices of the Climate Research Group of the Scripps Institution of Oceanography.

REFERENCES

Barnett, T. P., 1975: Discussion of climatic change in the northeast Pacific. Minutes of the 22nd Annual Eastern Pacific Oceanic Conference, Lake Arrowhead, Calif., 29 pp.

——, 1977: The principal time and space scales of the Pacific trade wind fields. *J. Atmos. Sci.* 34, 221–236.

Barton, E., A. Huyer and R. Smith, 1976: Temporal variation observed in the hydrographic regime near Cabo Corveiro in the northwest African upwelling region, Feb., Apr., 1974. *Deep-Sea Res.* (in press).

Bjerknes, J., 1961: El Niño study based on analysis of ocean surface temperatures, 1935–57. *Bull. Int. Amer. Trop. Tuna Comm.*, **5**, 219–303.

——, 1966a: Survey of El Niño, 1957–1958 in its relation to tropical Pacific meteorology. *Bull. Int. Amer. Trop. Tuna Comm.*, **12**, 3–62.

——, 1966b: The possible response of the atmospheric Hadley circulation to equatorial anomalies of ocean temperature. *Tellus*, **4**, 820–829.

Cromwell, T., and E. B. Bennett, 1959: Surface drift charts for the eastern tropical Pacific Ocean. *Bull. Intern. Amer. Trop. Tuna Comm.*, **3**, 215–237.

Davis, R., 1976: Predictability of sea surface temperature and sea level pressure anomalies over the North Pacific Ocean. *J. Phys. Oceanogr.*, **6**, 249–266.

Doberitz, R., 1967: Cross spectrum analysis of rainfall and sea temperature at the equatorial Pacific Ocean. *Bonner Meteor. Abhandl.* No. 8, Meteor. Inst., Univ. Bonn, 1–53.

EDS/NOAA, 1950–70: *Monthly Climatic Data for the World.* Environmental Data Service, NOAA, U. S. Dept. of Commerce.

Friehe, C., and K. Schmitt, 1977: Parameterizations of air-sea interface fluxes of sensible heat and moisture by the bulk aerodynamic formulas. *J. Phys. Oceanogr.*, **6**, 803–809.

Godfrey, J. S., 1975: An ocean spin-down, I: A linear experiment. *J. Phys. Oceanogr.*, **5**, 399–409.

Hickey, B., 1975: Relationship between fluctuations in sea level wind stress and sea surface temperature in the equatorial Pacific. *J. Phys. Oceanogr.*, **5**, 460–475.

Hires, R. I., and R. B. Montgomery, 1972: Navifacial temperature and salinity along track from Samoa to Hawaii, 1957–1965. *J. Mar. Res.*, **30**, 177–200.

Holladay, C., and J. O'Brien, 1975. Mesoscale variability of sea surface temperature. *J. Phys. Oceanogr.*, **5**, 761–772.

Hurlburt, H. E., J. C. Kindle and J. J. O'Brien, 1976: A numerical simulation of the onset of El Niño. *J. Phys. Oceanogr.*, **6**, 621–631.

Huyer, A., R. L. Smith and R. D. Pillsbury, 1974: Observations in a coastal upwelling region during a period of variable winds (Oregon Coast, July 1972). *Tethys*, **6**, 391–404.

Jenkins, G., and D. G. Watts, 1968: *Spectral Analysis and Its Applications.* Holden-Day, 515 pp.

Kendall, R., 1970: Pacific equatorial undercurrent. International Center for Environmental Research, Laguna Beach, Calif.

Knauss, J., 1959: Measurements of the Cromwell Current. *Deep-Sea Res.*, **6**, 265–286.

Kutzbach, J., 1967: Empirical igenvectors at sea level pressure, surface temperature and precipitation complexes over North America. *J. Appl. Meteor.*, **6**, 791–802.

Lighthill, M. J., 1969: Dynamic response of the Indian Ocean to onset of the southwest monsoon. *Phil. Trans. Roy. Soc. London*, **256**, 45–92.

Lorenz, E., 1958: Empirical orthogonal functions and statistical weather prediction. Rep. No. 1, Statistical Forecasting Project, Dept. Meteor., MIT.

McCreary, J., 1976: Eastern tropical ocean response to changing wind systems with application to El Niño. *J. Phys. Oceanogr.*, **6**, 634–645.

Miller, F. and M. Laurs, 1975: The El Niño of 1972–73 in the eastern Tropical Pacific Ocean. *Int. Trop. Tuna Comm. Bull.*, **16**, 403–417.

NOAA, 1974: *User's Guide to NODC's Data Services.* Environmental Data Service, NOAA, Washington, D. C.

NOS/NOAA, 1950–70: *Surface Water Temperature and Density, Pacific Coast, North and South America and Pacific Ocean Islands.* National Ocean Survey, NOAA. [Available from U. S. Govt. Printing Office.]

Namias, J., 1973: Response of the equatorial countercurrent to the subtropical atmosphere. *Science*, **181**, 1244–1245.

——, 1976: Some statistical and synoptic characteristics associated with El Niño. *J. Phys. Oceanogr.*, **6**, 130–138.

Ramage, C., 1975: Preliminary discussion of the meteorology of the 1972–73 El Niño. *Bull. Amer. Meteor. Soc.*, **56**, 234–242.

Reid, J. L., and A. W. Mantyla, 1976: The effect of the geostrophic flow upon coastal sea elevations in the northern North Pacific Ocean. *J. Geophys. Res.*, **81**, 3100–3110.

Schütte, K., 1967: Untersuchungen zur meteorologie und klimatologie des El Niño—Phänomens in Ecuador und Nordperu. *Bonner Meteor. Abhandl.*, **9**, p. 152.

Stevenson, M., and B. A. Taft, 1971: New evidence of the equatorial undercurrent east of the Galapagos Islands. *J. Mar. Res.*, **29**, 103–115.

——, O. Guillen and J. Santoro, 1969: *Marine Atlas of Pacific Coastal Water of South America*. University California Press.

Taft, B. A., and J. H. Jones, 1974: Measurements of the equatorial undercurrent in the eastern Pacific. *Progress in Oceanography*, Vol. 6, Pergamon Press, 47–110.

Tsuchiya, M., 1974: Variations of the surface geostrophic flow and eastern innertropical Pacific Ocean. *Fish. Bull.*, **72**, 1075–1086.

Wooster, W. S., 1960. El Niño. *Calif. Coop. Oceanic Fish. Invest. Rep.*, No. 7, 43–45.

——, and O. Guillen, 1974: Characteristics of the El Niño in 1972. *J. Mar. Res.*, **32**, 387–404.

Wyrtki, K., 1973: Teleconnections in the equatorial Pacific Ocean. *Science*, **180**, 66–68.

——, 1974a: Sea level and the seasonal fluctuations of the equatorial currents in the western Pacific Ocean. *J. Phys. Oceanogr.*, **4**, 91–101.

——, 1974b: Equatorial currents in the Pacific 1950 to 1970 and their relation to the Trade Winds. *J. Phys. Oceanogr.*, **4**, 372–380.

——, 1975: El Niño, the dynamic response of the equatorial Pacific Ocean to atmospheric forcing. *J. Phys. Oceanogr.*, **5**, 572–584.

——, 1977: Sea level during the 1972 El Niño. (Submitted to *J. Phys. Oceanogr.*)

——, and G. Meyers, 1975: The trade wind field over the Pacific Ocean, Part I, The mean field and the mean annual variation. Hawaii Institute of Geophysics, Rep. HIG-75-1, 1–25.

——, E. Stroup, W. Patzert, R. Williams and W. Quinn, 1976: Predicting and observing El Niño. *Science*, **191**, 343–346.